

Structured IQC Synthesis of Robust \mathcal{H}_2 Controllers in the Frequency Domain[★]

Maximilian Schütte^{*,**} Annika Eichler^{*,**} Herbert Werner^{**}

^{*} *Deutsches Elektronen-Synchrotron DESY, Germany
(e-mail: maximilian.schuette@desy.de).*

^{**} *Institute of Control Systems, Technical University Hamburg, Germany
(e-mail: h.werner@tuhh.de)*

Abstract: The problem of robust controller synthesis for plants affected by structured uncertainty, captured by integral quadratic constraints, is discussed. The solution is optimized towards a worst-case white noise rejection specification, which is a generalization of the standard \mathcal{H}_2 -norm to the robust setting including possibly non-LTI uncertainty. Arbitrary structural constraints can be imposed on the control solution, making this method suitable for distributed systems. The nonsmooth optimization algorithm used to solve the robust synthesis problem operates directly in the frequency domain, eliminating scalability issues for complex systems and providing local optimality certificates. The method is evaluated using a literature example and a real-world system using a novel implementation of a robust \mathcal{H}_2 -performance bound.

Keywords: Distributed robust controller synthesis, Numerical methods for optimal control, Controller constraints and structure, Complex systems, \mathcal{H}_2 -performance, IQCs

1. INTRODUCTION

In recent years, modern control has produced flexible and computationally efficient tools to analyze and synthesize controllers for plants affected by uncertainty from a variety of classes, from simple static unknown parameters to uncertain time delays and entirely non-linear dynamics. Current state-of-the-art methods include the use of integral quadratic constraints (IQCs) in combination with the Kalman–Yakubovich–Popov (KYP) lemma, see e.g. Veenman et al. (2016), which can be used not only to guarantee robust stability but at the same time also various performance bounds for uncertain closed-loop systems with fixed controllers. This and other linear matrix inequality (LMI) based methods, however quickly yield non-convex optimization problems in the synthesis case, possibly hardened by additional constraints on the controller structure such as output-feedback or decentralized control, which are often imposed by increasingly complex control applications. Solving these problems is either achieved by exploiting assumptions on the uncertainty, the interconnection structure, Eichler et al. (2014), using iterative methods, Veenman and Scherer (2014), or convex approximations, Furieri et al. (2020).

All these methods have downsides such as diminished applicability, increased conservatism or lack of optimality certificates, which is why in Cavalcanti and Simões (2020) a different approach is pursued. In this recent work, the authors use nonsmooth optimization techniques, see Apkarian and Noll (2006), to solve the IQC robust synthesis

problem directly in the frequency domain, thus yielding the full flexibility of the IQC framework along with local certificates of optimality and the ability to dictate the controller structure. The authors show that their method is directly compatible with existing nonsmooth optimization tools such as MATLAB’s SYSTUNE.

Among the commonly used performance specifications, \mathcal{H}_2 -performance is of particular interest to practitioners due to its inherent association with the closed-loop system’s ability to mitigate the influence of white Gaussian noise. An apparent shortcoming of the framework of Cavalcanti and Simões (2020) is therefore that it is not possible to formulate a robust \mathcal{H}_2 -performance problem with the current capabilities of SYSTUNE. After recapitulating the nonsmooth IQC optimization method in Section 2, the main contributions of this work hence lie in Section 3, where compatibility of the IQC framework and a robust \mathcal{H}_2 -performance test proposed by Paganini (1999) is shown, and in Section 4, where an efficient implementation of said test is outlined. Finally, in Section 5, we evaluate the method using an artificial example that highlights the performance benefit of the local optimality certificate, and a demanding real-world structured controller synthesis problem.

Notation. Let $\bar{\sigma}(X)$ denote the largest singular value of X . The bilinear sector transformation is given by $\text{sect}(X) = (I - X)(I + X)^{-1}$. The space of real rational proper transfer matrices without poles on the extended imaginary axis is denoted $\mathcal{RL}_\infty^{\bullet \times \bullet}$. Its subspace $\mathcal{RH}_\infty^{\bullet \times \bullet}$ contains those elements without poles in the closed right-half plane. $\mathcal{S}_\infty^{\times \bullet}$ is the subset of hermitian valued members of $\mathcal{RL}_\infty^{\bullet \times \bullet}$. Unless at risk of ambiguity, we will omit explicitly stating the dimensionality of spaces, operators and signals.

[★] The authors acknowledge support from Deutsches Elektronen-Synchrotron DESY Hamburg, Germany, a member of the Helmholtz Association HGF. © All figures and pictures under a CC BY 4.0 license.

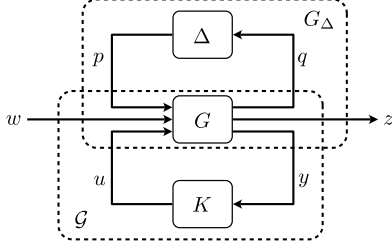


Fig. 1. Linear fractional representation of an uncertain system $\mathcal{G}(\Delta)$.

2. IQC SYNTHESIS VIA NONSMOOTH OPTIMIZATION

We consider an uncertain distributed system consisting of arbitrarily interconnected subsystems in standard linear fractional representation (LFR) as depicted in Figure 1 and described by

$$\begin{pmatrix} q \\ z \\ y \end{pmatrix} = G \begin{pmatrix} p \\ w \\ u \end{pmatrix}, \quad p = \Delta q, \quad u = Ky. \quad (1)$$

The uncertainty channel $p \rightarrow q$ is closed by the bounded causal operator $\Delta \in \mathbf{\Delta}$, where the compact set $\mathbf{\Delta}$ reflects the uncertainty in the system model and we require the common assumption that for $\rho \in [0, 1]$ also $\rho\Delta \in \mathbf{\Delta}$. The uncertain open-loop system G_Δ is given by the upper linear fractional transformation of its nominal LTI part G and Δ , $G_\Delta = \mathcal{F}_u(G, \Delta)$. Similarly, we have $\mathcal{G} = \mathcal{F}_l(G, K)$, where $K \in \mathbf{K}$ is a sought-after distributed output-feedback controller, whose required structure is encoded in the set of admissible dynamic controllers \mathbf{K} , that closes the control channel $y \rightarrow u$ and minimizes a worst-case performance criterion such as the \mathcal{H}_2 or \mathcal{H}_∞ -norm on the performance channel $w \rightarrow z$.

The IQC framework, Megretski and Rantzer (1997), provides a powerful tool for analyzing such interconnections for a broad range of uncertainties and finding suitable stabilizing and performance-optimizing controllers. We refer the reader to Veenman et al. (2016) for an in-depth treatment, but will in the following also introduce relevant parts of the theory in accordance with Cavalcanti and Simões (2020) required for the implementation and numerical results presented in subsequent sections.

We start by introducing multipliers $\Pi, \Pi_p \in \mathbf{\Pi}$ for the robustness and performance tests, respectively. The set of dynamic IQC multipliers $\mathbf{\Pi}$ imposes a virtually non-restrictive structure according to

$$\mathbf{\Pi} = \left\{ \Pi = \begin{pmatrix} \Sigma^H \Sigma & \phi_o^H \\ \phi_o & \Psi + \Psi^H \end{pmatrix} \right\}, \quad (2)$$

where $\Sigma, \phi_o, \Psi \in \mathcal{RL}_\infty$. Explicitly, we will mean these terms to constitute the so-called augmented multiplier $\Pi_a = \mathcal{C}(\Pi, \Pi_p)$, where the composition $\mathcal{C}: \mathbf{\Pi} \times \dots \times \mathbf{\Pi} \rightarrow \mathbf{\Pi}$ indicates block diagonal concatenation of the respective terms of its arguments, i.e. for

$$\Pi_i = \begin{pmatrix} \Sigma_i^H \Sigma_i & \phi_{o,i}^H \\ \phi_{o,i} & \Psi_i + \Psi_i^H \end{pmatrix}, \quad i \in \{1, 2\}$$

we get

$$\mathcal{C}(\Pi_1, \Pi_2) = \begin{pmatrix} \begin{bmatrix} \Sigma_1 & \Sigma_2 \end{bmatrix}^H \begin{bmatrix} \Sigma_1 & \Sigma_2 \end{bmatrix} & \begin{bmatrix} \phi_{o,1} & \phi_{o,2} \end{bmatrix}^H \\ \begin{bmatrix} \phi_{o,1} & \phi_{o,2} \end{bmatrix} & \begin{bmatrix} \Psi_1 & \Psi_2 \end{bmatrix} + \begin{bmatrix} \Psi_1 & \Psi_2 \end{bmatrix}^H \end{pmatrix}.$$

Note that Π and Π_p may themselves be constructed in the same fashion from smaller multipliers to match a block diagonal structure of Δ or to impose different performance criteria on contingent blocks of z , respectively. With this notation, we state the following robust analysis result adapted from Cavalcanti and Simões (2020):

Corollary 1. Consider interconnection (1) for a fixed $K \in \mathbf{K}$ s.t. $\mathcal{G} \in \mathcal{RH}_\infty$ and let $\Delta \in \mathbf{\Delta}$ be a bounded causal operator. Assume that:

- i) for all $\Delta \in \mathbf{\Delta}$, the interconnection (1) is well-posed;
- ii) for all $\Delta \in \mathbf{\Delta}$, the following IQC defined by some $\Pi \in \mathbf{\Pi}$ is satisfied

$$\int_{-\infty}^{\infty} \begin{pmatrix} \hat{q}(i\omega) \\ \hat{p}(i\omega) \end{pmatrix}^H \Pi(i\omega) \begin{pmatrix} \hat{q}(i\omega) \\ \hat{p}(i\omega) \end{pmatrix} d\omega \geq 0; \quad (3)$$

- iii) the condition

$$\bar{\sigma} \left(\text{sect} \left(- \begin{bmatrix} \phi_o(i\omega)\mathcal{G}(i\omega) + \Psi(i\omega) & 0 \\ \Sigma(i\omega)\mathcal{G}(i\omega) & -\frac{1}{2}I \end{bmatrix} \right) \right) < 1 \quad (4)$$

is satisfied for some $\Pi_p \in \mathbf{\Pi}$ and for all $\omega \in \mathbb{R}$, where

$$\begin{pmatrix} \Sigma^H \Sigma & \phi_o^H \\ \phi_o & \Psi + \Psi^H \end{pmatrix} = \mathcal{C}(\Pi, \Pi_p).$$

Then, the interconnection (1) is robustly stable and robust performance on the channel $w \rightarrow z$ w.r.t. the criterion

$$\int_{-\infty}^{\infty} \begin{pmatrix} \hat{z}(i\omega) \\ \hat{w}(i\omega) \end{pmatrix}^H \Pi_p \begin{pmatrix} \hat{z}(i\omega) \\ \hat{w}(i\omega) \end{pmatrix} d\omega \leq -\epsilon \|w\|^2 \quad (5)$$

is guaranteed.

Note that, as shown in Cavalcanti and Simões (2020), for multipliers of structure $\mathbf{\Pi}$, condition (4) implies the following frequency domain inequality, which is known from earlier works on IQC stability analysis. Letting $\Pi_a = \mathcal{C}(\Pi, \Pi_p)$,

$$\begin{pmatrix} \mathcal{G}(i\omega) \\ I \end{pmatrix}^H \Pi_a(i\omega) \begin{pmatrix} \mathcal{G}(i\omega) \\ I \end{pmatrix} \leq -\epsilon I \quad \forall \omega \in \mathbb{R}. \quad (6)$$

With this modification, the search for a feasible multiplier Π_a can be performed directly in the frequency domain using nonsmooth optimization techniques such as Apkarian and Noll (2006), without having to resort to frequency gridding. The advantages over using the KYP lemma to obtain an equivalent LMI condition for (6) without gridding are manifold:

- 1) No Lyapunov variables need to be introduced, which scale quadratically with system size and pose computational limitations for large systems.
- 2) No semi-definite program (SDP) solvers are required to solve any LMIs. These tend to struggle with numerical issues when the involved matrices are badly conditioned and may falsely report an infeasible solution as feasible, posing risks if the result is not verified. Bad conditioning can be an outcome of transformations needed to render the problem convex, see e.g. Schütte et al. (2022).

- 3) Non-convex problems (e.g. synthesis) can be directly solved. For the LMI approach, iterative methods, e.g. Veenman and Scherer (2014), that cannot provide even local optimality certificates and produce often undesirable high-order controllers need to be used instead, increasing conservatism.
- 4) Structural constraints on the controller design are easily incorporated.
- 5) Poles of the basis functions for dynamic multipliers need not be selected a priori but are optimized by the optimization algorithm.

Possible downsides of the frequency domain approach are addressed in Section 5.

3. ROBUST \mathcal{H}_2 -PERFORMANCE

The issue of robust \mathcal{H}_2 -performance in the sense of $\sup_{\Delta \in \Delta} \|\mathcal{G}_\Delta\|_2$ is not trivial and has been discussed from various viewpoints in the literature. Noteworthy contributions include Stoerovogel (1993), Paganini (1996), Feron (1997) and Sznaier et al. (2002). A survey is given in Paganini and Feron (2000) and the topic is subject to ongoing research, see e.g. Chamanbaz et al. (2020). Despite the appealing nature of this performance metric from an engineering perspective, $\mathcal{H}_\infty/\mathcal{H}_2$ -control, guaranteeing \mathcal{H}_2 -performance only for the nominal plant and performing the worst-case analysis in terms of an \mathcal{H}_∞ specification, has emerged as a popular choice due to its simplicity, Sznaier et al. (2002). Complications in the mathematical treatment of \mathcal{H}_2 -criteria arise particularly in the case of non-LTI uncertainties, where the classical definition of the \mathcal{H}_2 -norm is not applicable and the interpretations of the \mathcal{H}_2 -performance in terms of the impulse response of a system and its ability to reject white noise diverge, see Paganini and Feron (2000). The case of white noise rejection is further complicated by the stochastic nature of the disturbance source and has strategically been adapted in Paganini (1996) by considering a worst-case analysis over a set of deterministic white signals $W_{\eta,B} \subset \mathcal{L}_2^\bullet$ instead, resulting in the semi-norm $\|\cdot\|_{W_{\eta,B}}$. These signals are characterized by having a flat spectrum with accuracy η up to bandwidth B and may taper off thereafter. Although it was shown that, quantitatively, the bound obtained from the white noise rejection approach can be greater than the bound obtained from the impulse response approach,

$$\|\mathcal{G}(\Delta)\|_{2,\text{ir}} \leq \|\mathcal{G}(\Delta)\|_{2,\text{wn}},$$

it is important to keep in mind that these interpretations are no longer equivalent, i.e. neither choice is inherently superior. We adopt the white noise rejection interpretation going forward with

$$\|\mathcal{G}_\Delta\|_{2,\text{wn}} := \lim_{\substack{\eta \rightarrow 0+ \\ B \rightarrow \infty}} \|\mathcal{G}_\Delta\|_{W_{\eta,B}} \quad (7)$$

since its definition in terms of signals with particular spectral properties is more natural to the frequency domain approach pursued in this work. Furthermore, the computation of a bound on $\|\mathcal{G}(\Delta)\|_{2,\text{ir}}$ requires solving an algebraic Riccati equation and is therefore susceptible to similar computational scalability issues previously discussed for the KYP lemma. Nevertheless, we note that, as shown in Paganini and Feron (2000), the impulse response method weakly exploits the necessary causality of Δ , which will in

general lead to less conservative bounds compared to the white noise rejection approach.

We now show how the result of Paganini (1999) may be transferred to the IQC framework.

Corollary 2. For $Y \in \mathcal{S}_\infty$ and of finite order, the multiplier

$$\Pi_p = \begin{pmatrix} I & 0 \\ 0 & -Y \end{pmatrix} \quad (8)$$

in conjunction with Corollary 1 guarantees robust worst-case \mathcal{H}_2 -performance γ on the channel $w \rightarrow z$ of interconnection (1) with

$$\|\mathcal{G}_\Delta\|_{2,\text{wn}} \leq \frac{1}{2\pi} \int_{-\infty}^{\infty} \text{trace}(Y(i\omega)) d\omega < \gamma^2. \quad (9)$$

Proof. First note that $\Pi_p \in \Pi$, so Corollary 1 applies. Further, since $Y(s) \in \mathcal{S}_\infty$ and of finite order, its frequency response $Y(i\omega)$ is of bounded variation and there exists a monotonically decreasing function $g \in \mathcal{L}_1(\mathbb{R}_+)$ such that

$$0 \leq Y(i\omega) \leq g(|\omega|)I, \quad (10)$$

where the first inequality holds as a consequence of (6). It is then straightforward to show that the sufficiency part of Theorem 6 in Paganini (1999) deriving the bound (9) and its extensions to multivariable noise and nonlinear uncertainties also hold for $Y(s = i\omega)$.

4. IMPLEMENTATION

To synthesize a performance-optimized, robust and structured controller, we first formulate a parameterized optimization problem based on the theory in Sections 2 and 3 that can be solved with standard optimization algorithms. In this work, we rely on the nonsmooth optimization algorithm by Apkarian and Noll (2006) and its implementation in the **SYSTUNE** function from the MATLAB Control System Toolbox, The MathWorks Inc. (2021).

Problem 3. Given interconnection (1) well-posed for all $\Delta \in \Delta$,

$$\underset{\chi}{\text{minimize}} \quad \frac{1}{2\pi} \int_{-\infty}^{\infty} \text{trace}(Y(i\omega, \chi)) d\omega \quad (11)$$

$$\text{subject to} \quad \mathcal{G}(s, \kappa) \text{ stable,} \\ \max_{\omega} \bar{\sigma}(\text{sect}(-\mathcal{P}(s, \chi, \kappa))) < 1, \quad (12)$$

$$h(\chi) \leq 0, l(\kappa) \leq 0. \quad (13)$$

where $\mathcal{G}(s, \kappa) = \mathcal{F}_l(G(s), K(s, \kappa))$ and

$$\mathcal{P}(s, \chi, \kappa) = \begin{bmatrix} \phi_o(i\omega, \chi)\mathcal{G}(i\omega, \kappa) + \Psi(i\omega, \chi) & 0 \\ \Sigma(i\omega, \chi)\mathcal{G}(i\omega, \kappa) & -\frac{1}{2}I \end{bmatrix}. \quad (14)$$

Equations (11) and (12) stem from Corollary 1 and Corollary 2, respectively. χ and κ are real parameter vectors for the multiplier and controller variables, respectively, and we require that $\Pi_a(s, \chi) \in \Pi$ and $K(s, \kappa) \in \mathcal{K}$ are smooth in their respective parameters. The functions $h(\cdot)$ and $l(\cdot)$ serve as constraints on the parameter vectors that can, for example, be used to ensure (3) holds, i.e. Π a-priori satisfies the IQC for a given class of uncertainty, or to further shape the set of admissible controllers \mathcal{K} in addition to the structural dependence of K on κ .

As of version 10.11 of the MATLAB Control System Toolbox, the **SYSTUNE** function does not support tuning goals of the form (11). The results presented in Section 5 were

produced with an experimental implementation where we extended the **SYSTUNE** code with the required functionality for a specific but nevertheless versatile parameterization for $Y(s)$ adapted from Jonsson and Megretski (1999):

$$Y(s, \chi) = \Psi_Y(s, \chi) + \Psi_Y(s, \chi)^H$$

$$\Psi_Y(s, \chi) = \sum_{i=1}^N \frac{X_i s + X_i a_i + Z_i b_i}{s^2 + 2a_i s + a_i^2 + b_i^2}. \quad (15)$$

Here X_i and Z_i are real matrices and $a_i \in \mathbb{R}_+$ and $b_i \in \mathbb{R}$ are scalars that determine the real and imaginary parts of the pole location of each summand, respectively. As such, as long as all a_i, b_i are distinct, $\Psi_Y(s, \chi)$ is the most general way to parameterize an N^{th} -order transfer matrix in \mathcal{RH}_∞ . The parameter vector χ of $Y(s, \chi)$ is just the concatenation of the vectorized values X_i, Z_i, a_i, b_i .

In order to add a new tuning goal for **SYSTUNE**, an evaluation of the objective function (11) and its gradient in terms of its parameters has to be implemented. While numerical methods can be used here, the parameterization (15) admits an elegant analytical solution.

Lemma 4. Given parameterization (15) for $Y(s, \chi)$, it holds that

$$\frac{1}{2\pi} \int_{-\infty}^{\infty} \text{trace}(Y(i\omega, \chi)) d\omega = \sum_{i=1}^N \text{trace}(X_i). \quad (16)$$

Proof. Following the arguments in Jonsson and Megretski (1999), we find for each summand in (15) that, for $b_i = 0$,

$$\begin{aligned} \lim_{B \rightarrow \infty} \int_{-B}^B \frac{X_i s + X_i a_i + Z_i b_i}{s^2 + 2a_i s + a_i^2 + b_i^2} d\omega \\ = \lim_{B \rightarrow \infty} \int_{-B}^B \frac{X_i}{i\omega + a_i} d\omega \\ = \lim_{B \rightarrow \infty} 2X_i \arctan\left(\frac{B}{a_i}\right) = \pi X_i. \end{aligned} \quad (17)$$

By analytic continuation of the function $\int_{-B}^B \frac{1}{i\omega + z} d\omega$ in the region $\text{Re } z > 0$, (17) holds for all $a_i > 0$, $b_i \in \mathbb{R}$. It follows that

$$\begin{aligned} \frac{1}{2\pi} \int_{-\infty}^{\infty} \text{trace}(Y(i\omega, \chi)) d\omega \\ = \frac{1}{\pi} \lim_{B \rightarrow \infty} \int_{-B}^B \text{trace}(\Psi_Y(i\omega, \chi)) d\omega \\ = \sum_{i=1}^N \text{trace}(X_i). \end{aligned} \quad (18)$$

The gradient $\frac{d}{d\chi} \frac{1}{2\pi} \int_{-\infty}^{\infty} \text{trace}(Y(i\omega, \chi)) d\omega$ is consequently easily computed as well - it is just one for every diagonal element of any X_i and zero otherwise. At this point, it may seem that in contrast to advantage 5, the other parameters including the pole and zero locations are not optimized, as they do not appear in the gradient. This however is not the case, as these parameters are still part of the hard constraint (12).

Still, with respect to the conservatism of this method, we point out that unlike the frequency gridding approach used in Paganini and Feron (1997), the finite-order parameterization (15) of $Y(s)$ cannot achieve tightness at all frequencies.

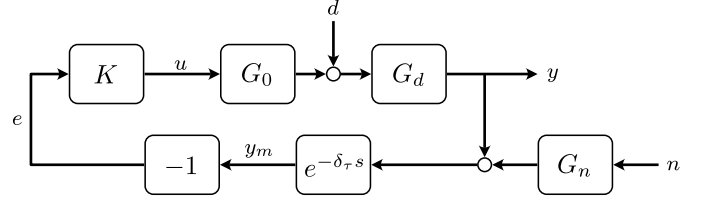


Fig. 2. Demo system with parametric and measurement time delay uncertainty.

5. DISCUSSION & RESULTS

To evaluate the practical use and limitations of the proposed method, we solve Problem 3 for a simple artificial plant and a complex real-world system.

5.1 4th-Order MISO System with Uncertain Natural Frequency and Measurement Time Delay

This example, inspired by Veenman and Scherer (2014) and depicted in Figure 2, studies the robust control of a plant with arbitrarily fast time-varying natural frequency given by

$$G_0(s, \delta) = \frac{4}{s^2 + 0.1(1 + 0.5\delta) + (1 + 0.5\delta)^2}, \quad (19)$$

where $\delta \in \Delta_{\text{ltv, re, dr}}$ with $|\delta| \leq 1$ and $|\dot{\delta}|$ unbounded. It is followed by an output disturbance modeled by

$$G_d(s) = \frac{10}{s + 0.1}. \quad (20)$$

The output measurement delay $\delta_\tau \in [0, 0.025]$ is considered constant. As such, this uncertainty is of type $\Delta_{\text{ltv, rb, td}}$ and we use the corresponding multiplier from the library of Cavalcanti and Simões (2020). Instead of the original mixed-sensitivity problem, we adapt the example to an output regulation problem, i.e. we are interested in keeping the output at zero under the influence of white noise at the disturbance and measurement noise inputs. The latter was added in place of the reference input and is filtered by

$$G_n(s) = \frac{s}{s + 10} \quad (21)$$

to achieve the typical high-pass characteristic of measurement noise. As such the system caters nicely to the robust \mathcal{H}_2 -performance problem. After LFR decomposition into the form of Figure 1, the uncertainty Δ is composed as

$$\Delta = \begin{pmatrix} \delta I_3 & 0 \\ 0 & \delta_\tau \end{pmatrix}. \quad (22)$$

The uncertainty $\delta I_3 \in \Delta_{\text{ltv, re, dr}}$ is captured by the constant multiplier

$$\Pi(s) = \begin{pmatrix} D^H D & W^H \\ W & -D^H D \end{pmatrix}, \quad (23)$$

where $D \in \mathbb{R}^{3 \times 3}$ and

$$W = \begin{pmatrix} 0 & W_{12} & W_{13} \\ -W_{12} & 0 & W_{23} \\ -W_{13} & -W_{23} & 0 \end{pmatrix} \in \mathbb{R}^{3 \times 3}, \quad (24)$$

the particular structure of which is enforced with constraint (13).

Figure 3 shows the impulse responses of a third-order controller synthesized using **SYSTUNE** for the nominal plant without measurement delay and of a third-order robust

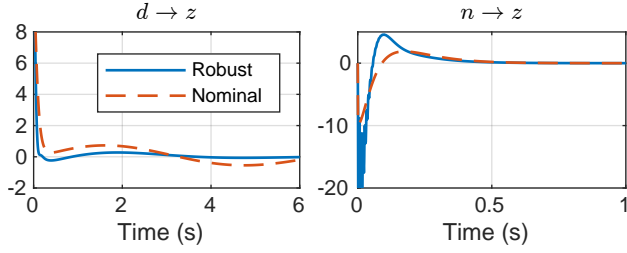


Fig. 3. Impulse responses for the system in Figure 2 for a nominal and a robust controller of third order.

controller synthesized using Problem 3 when applied to a Padé-approximation of the system for $\delta = -1$ and $\delta_r = 0.025$. The nominal controller achieves a \mathcal{H}_2 -norm of 4.58, whereas the robust controller achieves 4.16, an improvement of 9%. This is in fact the worst performance for both controllers that was found over a grid scan of δ and on average, the nominal controller actually performs better by 17%. This however is purely empirical and no hard guarantee can be provided, whereas the robust controller provides a guaranteed worst-case bound of 6.85.

5.2 Decentralized Control for an Optical Synchronization System with Uncertain Dampings

Finally, the full flexibility of this controller synthesis method is demonstrated using a real-world control problem for a complex decentralized system. The laser-based optical synchronization (LbSync) system, Schulz et al. (2015), developed at Deutsches Elektronen-Synchrotron (DESY), is used to transport an ultra-stable timing reference signal across a large-scale facility from a common root via intermediate oscillators to multiple end stations, creating a network of phase-locked loops (PLLs) with local controllers. Using mode-locked lasers as tunable optical oscillators allows high-bandwidth locking to optical or RF reference signals and the bidirectional property of optical fibers allows for an autocorrelation scheme, with which the propagation time on the transmission line can be stabilized against environmental disturbances. With these techniques, a timing synchronization of sub 10 fs RMS can be achieved over multiple kilometers, which has been demonstrated in the case of the European X-Ray Free-Electron Laser photon-science facility in Hamburg, Germany, Schulz et al. (2019).

The associated control problem was classified as a decentralized, fixed-order, output-feedback problem in Schütte et al. (2021) and extended with robustness guarantees in Schütte et al. (2022). To compare the LMI synthesis method used in the latter work, which is based on convexification and transformation of the original problem which can then be solved with a single SDP, we apply the frequency domain method of Section 4 to the same model of the LbSync system that was used before. In this baseband model, a reference signal produced by an RF oscillator is transferred to the optical domain using a first laser, repeated using a second laser for increased transmission distance, and finally used to synchronize an experimentation laser. As the phase-noise of each oscillator is independent, this yields a four-input, single-output system of 24th-order, where the output is given as the phase error between the reference and the experimentation laser.

Table 1. Comparison of the LMI and frequency domain synthesis solutions.

Test	LMI	Freq.-Domain	Rel. Impr.
Robust \mathcal{H}_2 -perf. bound	29.154	9.908	66.0 %
Average \mathcal{H}_2 -perf. ^a	7.792	7.185	7.8 %
Worst \mathcal{H}_2 -perf. ^a	8.031	7.324	8.8 %
Gap	21.123	2.584	87.8 %
Relative gap	263 %	35.3 %	86.6 %
Comp. time per iter. ^b	2.48 s	33.21 s	

^a 10 000 uncertainty samples

^b 3.6 GHz six-core processor

Further details on the involved models are given in Schütte et al. (2022). The uncertainty is of class $\Delta_{\text{ltv, re, dr}}$ and comprises independent uncertain dampings in the piezoelectric actuators used to tune each of the lasers. We note that the uncertainty classes that can be treated with the full-block multiplier approach used in Schütte et al. (2022) is limited compared to the more general IQC framework incorporated in this work, e.g. the example of Section 5.1 is not covered because of the uncertain time delay.

The goal is to synthesize feedback gains for the individual PLLs locking the laser oscillators to their respective references that minimizes the robust \mathcal{H}_2 -norm of the closed loop system. For dampings in the range $\delta_i \in [0.1, 0.3]$, results and statistics are collected in Table 1. Besides an improvement of the worst-case nominal LTI \mathcal{H}_2 -performance $\sup_{\Delta \in \Delta} \|\mathcal{G}_\Delta\|_2$ of almost 10 %, a clear advantage of the frequency domain method appears to be the significantly reduced gap between the provided bound on the robust performance and its statistically estimated actual quantity of over 85 %. It is important to note at this point, with respect to the discussion in Section 3, the bound provided by the LMI approach is of the impulse-response type and therefore not strictly equivalent to the worst-case white noise rejection analysis result of the frequency domain approach. We also recall that the LMI bound is computed only for a convexified version of the original problem, explaining the increased conservatism compared to the solution obtained from the nonsmooth optimization algorithm, which provides at least a local optimality certificate. An apparent disadvantage of the frequency domain method is its significantly increased computation time. Multiple comments are in order regarding this observation.

- 1) To get a fair comparison, both computations were executed on the same machine, but we also had success running the modified SYSTUNE code parallelized on a high-performance computing cluster, greatly reducing the computation time.
- 2) To reduce the number of random initial iterates, a hot-start technique may be considered, where a nominal controller is first synthesized and then randomly perturbed versions are used as initial points for the robust synthesis problem.
- 3) The order of the discussed problem is still relatively low. Scaling issues of the LMI approach are only expected to be a significant issue until the problem size exceeds a few hundred states, at which point the frequency domain method is expected to get the upper hand in terms of computational complexity.

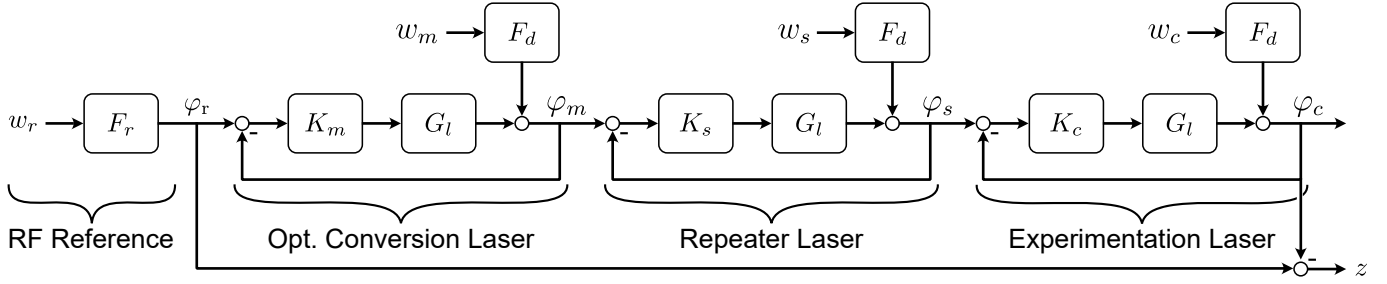


Fig. 4. Block diagram of the LbSync system.

6. CONCLUSION

In this paper, we demonstrated the successful application of a frequency domain \mathcal{H}_2 -performance bound to robust controller synthesis by formulating a corresponding IQC problem which is then solved using nonsmooth optimization. We proposed a suitable parameterization for the bounding multiplier which allows the bound and its gradient to be efficiently evaluated and used this to extend the applicability of MATLAB's SYSTUNE function to robust \mathcal{H}_2 synthesis for a wide range of uncertainties. We evaluated this method using a modified literature example and verified the generated solutions using industry-standard robust analysis methods. We found that, using a moderate number of random initial parameters, robust controllers that outperform nominal solutions for certain uncertainty realizations could be synthesized. At the same time, we demonstrated the flexibility of the method in dealing with uncertainties from a wide range of classes. Finally, we applied the method to a complex real-world distributed system and found that, compared to a previously used LMI synthesis method, the conservatism induced by using finite-order parameterizations for the \mathcal{H}_2 -performance multiplier was significantly lower than the conservatism stemming from a convexification of the optimization problem for LMI-based synthesis.

REFERENCES

- Apkarian, P. and Noll, D. (2006). Nonsmooth \mathcal{H}_∞ Synthesis. *IEEE Trans. Autom. Control*, 51(1), 71–86.
- Cavalcanti, V.M.G.B. and Simões, A.M. (2020). IQC-synthesis under structural constraints. *Int. J. Robust Nonlinear Control*, 30(13), 4880–4905.
- Chamanbaz, M., Sznaier, M., Lagoa, C., and Dabbene, F. (2020). Probabilistic Discrete Time Robust \mathcal{H}_2 Controller Design. In *Proc. 59th IEEE Conf. Decis. Control*, 2240–2245.
- Eichler, A., Hoffmann, C., and Werner, H. (2014). Robust control of decomposable LPV systems. *Automatica*, 50(12), 3239–3245.
- Feron, E. (1997). Analysis of Robust \mathcal{H}_2 Performance Using Multiplier Theory. *SIAM J. Control Optim.*, 35(1), 160–177.
- Furieri, L., Zheng, Y., Papachristodoulou, A., and Kamgarpour, M. (2020). Sparsity Invariance for Convex Design of Distributed Controllers. *IEEE Trans. Control Netw. Syst.*, 7(4), 1836–1847.
- Jonsson, U. and Megretski, A. (1999). IQC characterizations of signal classes. In *Proc. 1999 Eur. Control Conf.*, 1481–1486.
- Megretski, A. and Rantzer, A. (1997). System analysis via integral quadratic constraints. *IEEE Trans. Autom. Control*, 42(6), 819–830.
- Paganini, F. (1996). A set-based approach for white noise modeling. *IEEE Trans. Autom. Control*, 41(10), 1453–1465.
- Paganini, F. (1999). Convex methods for robust \mathcal{H}_2 analysis of continuous-time systems. *IEEE Trans. Autom. Control*, 44(2), 239–252.
- Paganini, F. and Feron, E. (1997). Analysis of robust \mathcal{H}_2 performance: comparisons and examples. In *Proc. 36th IEEE Conf. Decis. Control*, 1000–1005.
- Paganini, F. and Feron, E. (2000). Linear Matrix Inequality Methods for Robust \mathcal{H}_2 Analysis: A Survey with Comparisons. In L. El Ghaoui and S.I. Niculescu (eds.), *Advances in Linear Matrix Inequality Methods in Control*, 129–151. SIAM, Philadelphia, PA, USA.
- Schulz, S. et al. (2015). Femtosecond all-optical synchronization of an X-ray free-electron laser. *Nat. Commun.*, 6, 5938.
- Schulz, S. et al. (2019). Few-Femtosecond Facility-Wide Synchronization of the European XFEL. In *Proc. 39th Int. Free-Electron Laser Conf.*, 318–321.
- Schütte, M., Eichler, A., Schlarb, H., Lichtenberg, G., and Werner, H. (2021). Decentralized Output Feedback Control using Sparsity Invariance with Application to Synchronization at European XFEL. In *Proc. 60th IEEE Conf. Decis. Control*, 5723–5728.
- Schütte, M., Eichler, A., Schlarb, H., Lichtenberg, G., and Werner, H. (2022). Convex Synthesis of Robust Distributed Controllers for the Optical Synchronization System at European XFEL. In *Proc. 6th IEEE Conf. Control Technol. App.*
- Stoorvogel, A.A. (1993). The robust \mathcal{H}_2 control problem: a worst-case design. *IEEE Trans. Autom. Control*, 38(9), 1358–1371.
- Sznaier, M., Amishima, T., Parrilo, P.A., and Tierno, J. (2002). A convex approach to robust performance analysis. *Automatica*, 38(6), 957–966.
- The MathWorks Inc. (2021). MATLAB: Control System Toolbox.
- Veenman, J. and Scherer, C.W. (2014). IQC-synthesis with general dynamic multipliers. *Int. J. Robust Nonlinear Control*, 24(17), 3027–3056.
- Veenman, J., Scherer, C.W., and Köroğlu, H. (2016). Robust stability and performance analysis based on integral quadratic constraints. *Eur. J. Control*, 31, 1–32.